Genes & Diseases (2022) 9, 201–215

Available online at www.sciencedirect.com

ScienceDirect

journal homepage: http://ees.elsevier.com/gendis/default.asp

FULL LENGTH ARTICLE

Comparison of hepatic gene expression profiles between three mouse models of Nonalcoholic Fatty Liver Disease

Liping Xiang [a], Yang Jiao [a], Yiling Qian [a,b], Yao Li [c], Fei Mao [a,], Yan Lu [a,*]**

[a] *Department of Endocrinology and Metabolism, Zhongshan Hospital, Fudan University, Shanghai 200032, PR China*
[b] *Department of Endocrinology and Metabolism, Minhang Branch, Zhongshan Hospital, Central Hospital of Minhang District, Shanghai Minhang Hospital, Fudan University, Shanghai 200032, PR China*
[c] *Department of Laboratory Animal Science, Shanghai Jiao Tong University School of Medicine, Shanghai 200025, PR China*

Received 24 December 2020; received in revised form 6 February 2021; accepted 17 February 2021
Available online 27 February 2021

KEYWORDS
DEGs;
Murine models;
NAFLD;
Pathway analysis;
Transcriptome

Abstract Non-alcoholic fatty liver disease (NAFLD) has become the most common chronic liver disorder worldwide. Murine models of NAFLD have been widely used to explore its pathogenesis. In this study, we performed a systematic evaluation of hepatic genome-wide mRNA expression by RNA-Sequencing using three mouse models of NAFLD: leptin receptor deficient db/db mice, high-fat high-sugar diet (HSHF)-induced obese mice, and dexamethasone (DEX)-induced NAFLD mice. As a result, we found both distinct and common pathways in the regulation of lipid metabolism from transcriptomes of three mouse models. Moreover, only a total of 12 differentially expressed genes (DEGs) were commonly detected among all three mouse groups, indicating very little overlap among all three models. Therefore, our results suggest that NAFLD is a heterogeneous disease with highly variable molecular mechanisms.

* Corresponding author.
** Corresponding author.
E-mail addresses: medichem@126.com (F. Mao), lu.yan2@zs-hospital.sh.cn (Y. Lu).
Peer review under responsibility of Chongqing Medical University.

https://doi.org/10.1016/j.gendis.2021.02.008

Introduction

Nonalcoholic fatty liver disease (NAFLD) has become the leading cause of liver damage and dysfunction worldwide and is strongly associated with metabolic diseases.[1] The spectrum of NAFLD ranges from simple steatosis to nonalcoholic steatohepatitis (NASH) and end-stage liver diseases.[1] The pathogenesis of NAFLD is multi-factorial and triggered by various environmental factors in the context of a genetic predisposition.[2,3]

Murine models are important platforms to investigate a deep mechanistic understanding and test therapeutic interventions for human diseases. Most common mouse models of NAFLD widely used are diet-induced models, including high fat diet,[4] high fructose diet.[5] Besides, leptin receptor deficient db/db mice, is also a frequently used obese model, which develop hepatic steatosis.[6,7] Moreover, stress induced increased glucocorticoid levels also play a critical role in the development of NAFLD.[8] Indeed, dexamethasone (DEX), a class of frequently prescribed drugs for anti-inflammation in patients, is associated with metabolic side-effects, including dyslipidemia and hepatic steatosis.[8] Overall, the cause of NAFLD could be heterogeneous, while current published research is not enough to elucidate its exact mechanisms. Therefore, classifying the cause of NAFLD and its underlying molecular mechanism could help to gain better understanding into its pathogenesis and identify potential therapeutic targets for its treatment.

Transcriptomic analysis provide a technically and theoretically well-developed global method for the comparison of different murine pathway activation, which may provide a reasonable proxy for such analysis.[9,10] Over the past decade, several microarray profiling studies have been performed to investigate specific aspects of NAFLD biology.[11,12,13] However, very few studies have ever simultaneously investigated the full spectrum of fatty liver disease, or performed a comparison between different mouse models. In the present study, we performed a systematic transcriptome-wide analysis of three murine models of NAFLD, including a typical high sugar high fat diet induced NAFLD (HSHF), a dexamethasone-induced NAFLD (DEX), as well as leptin-receptor deficient mice (db/db). We analyzed the biological function of dysregulated genes (DEGs) and associated pathways in each mouse model of NAFLD. Based on these results, we aim to provide novel insights into the molecular characteristics and pathways of NAFLD pathogenesis, and potential therapeutic targets for its treatment.

Materials and methods

Animal experiments

All of animal experiments were approved by the Institutional Care and Use Committee at Shanghai Jiao Tong University School of Medicine with the "Guide for the Care and Use of Laboratory Animals" published by the National Institutes of Health. Wild-type male C57BL/6J mice at the age of 8 weeks were purchased from Shanghai Laboratory Animal Company (SLAC). Male db/db mice aged 8 weeks were purchased from the Nanjing Biomedical Research Institute of Nanjing University (Nanjing, China). One day after arrival, they were habituated for 1 week for regular chow. All mice were housed at 21 °C ± 1 °C with 55% ± 10% humidity and a 12-h light/12-h dark cycle. HSHF group of 8 week old male C57BL/6J mice received a high-sucrose/high fat diet (HSHF diet; 45 kcal% fat, 17 kcal% sucrose) for 12wks as described.[14] For DEX treatment, 8-week old male C57BL/6J mice received 2 weeks of dexamethasone (1 mg/kg; Sigma Aldrich, St. Louis, MO) or vehicle (0.25% PEG400, 0.25% Tween20 in ddH_2O) treatment via subcutaneous injection.

Sample collection

Mice were anesthetized with sodium-pentobarbital (Nembutal, 80 mg/kg, ip). The abdominal cavity was opened and blood was withdrawn from the inferior vena cava. The liver was then perfused through the portal vein with ice-chilled saline. Liver from the left lobe was harvested and snap frozen in liquid nitrogen.

Liver triacylglycerol assay

For liver triacylglycerol assay, hepatic tissues (~100 mg) were homogenized in 50 mM NaCl. The homogenate (500 μl) was mixed with chloroform/methanol (2:1, 4 ml) and incubated overnight at room temperature with gentle shaking. Homogenates were vortexed and centrifuged for 5 min at 3000 g. The lower lipid phase was collected and concentrated. The lipid pellets were dissolved in 1% Triton X100 in phosphate-buffered saline, and hepatic triacylglycerol content was determined via enzymatic colorimetric methods.

RNA extraction and transcriptome sequencing

Approximately 5 mg of frozen liver powder was completely dissolved in 500 μl of TRIzol reagent at room temperature. Total RNA was extracted with TRIzol (Invitrogen, Carlsbad, CA, USA) according to the manufacturer's protocol. The quality of total RNA was assessed by the Agilent Bioanalyzer 2100 (Santa Clara, CA, USA). RNA libraries were constructed by using rRNA-depleted RNAs with TruSeq Stranded Total RNA Library Prep Kit (Illumina, San Diego, CA, USA) according to the manufacturer's instructions. Libraries were controlled for quality and quantified using the BioAnalyzer 2100 system (Agilent Technologies, Inc., USA). 10 pM libraries were denatured as single-stranded DNA molecules, captured on Illumina flow cells, amplified *in situ* as clusters and finally sequenced for 150 cycles on Illumina HiSeq Sequencer according to the manufacturer's instructions.

Data processing and analysis

Paired-end reads were harvested from Illumina HiSeq 4000 sequencer, and were quality controlled by Q30. After 3' adaptor-trimming and low quality reads removing by cutadapt software (v1.9.3), the high quality clean reads were aligned to the reference genome (UCSC MM10) with hisat2 software (v2.0.4). Then, guided by the Ensembl GTF gene annotation file, cuffdiff software (part of cufflinks) was

used to get the gene level FPKM as the expression profiles of mRNA, and fold change and *P*-value were calculated based on FPKM, differentially expressed mRNA were identified. GO (Gene Ontology) and KEGG Pathway (Kyoto Encyclopeida of Genes and Genomes) enrichment analysis were performed based on the differentially expressed mRNAs. FPKM values were calculated to normalize read counts. Based on FPKM of each gene of each sample, the squares of Pearson coefficient r values were calculated to show correlations between samples and reproducibility. FPKM of each gene was averaged in each group, and $\log_2$ (FPKM+1) values were used to generate a heatmap, in which groups and genes were clustered, respectively. The Euclidean distances between groups were also calculated based on $\log_2$ (FPKM+1) of all genes. Differentially expressed genes were annotated and classified with GO and KEGG terms by using the R clusterprofile package.

Statistical analysis

Data were expressed as mean ± S.E.M. Student's *t* test was performed to evaluate significant differences between the compared groups, which were defined as $P < 0.05$.

Results

RNA-Seq data validation

As shown in Table 1, in this study, we included three different mouse models, including dexamethasone treated group (DEX) and high sugar high fat induced NAFLD group (HSHF), as well as leptin receptor-deficient obese group (db/db), with two to four replicates for each group. As expected, we observed a significant elevation of hepatic triglyceride contents in all three mouse models of NAFLD (Fig. S1). The reproducibility and reliability of these data sets are demonstrated in Fig. S2, showing that gene expression reads as fragments per kilobase of transcript per million mapped reads (FPKM) 3 of all samples in three groups were well-correlated. Pearson correlation r values between all samples in three groups are listed in Table S1, all well correlated. The correlation coefficient matrix of all samples shown in Fig. S3 demonstrates clear patterns, confirming that all of the data within each group were well-correlated. Principal correlation analysis (PCA) of all three groups also showed samples within each group shared similarities (Fig. S3). These data demonstrated that all of the RNA-Seq results obtained were reproducible and reliable.

Table 1 Group information of three mouse models of NAFLD used in the study.

Group	Strain	Treatment	Number of samples (*n*)
			CON *vs.* Treatment
1	C57BL6/J WT	DEX for 2wks	4 *vs.* 4
2	C57BL6/J WT	HSHF for 12wks	2 *vs.* 2
3	C57BL6/J *db/db*	/	4 *vs.* 4

Genome-wide gene expression and clustering analysis

We then carried out hierarchical clustering analysis of gene expressions in the livers of all three different groups. Normalized gene counts were detected after batch-effect correction by IQR (Inter-Quartile Range) boxplot and PCA analysis to confirm it's well normalized with no obvious bias in each group (Fig. 1A, B). Normalized gene counts were further calculated and plotted in a heatmap (Fig. 1C), which shows different gene expression patterns among three different groups. To quantify the differentially expressed genes, we used the Cutdiff to compare the expression level of each gene in each group of different treatment *vs.* WT C57BL/6J mice and plotted log10 (p.adj) versus log2 (-fold change).

Differential expression analysis of RNA transcripts from the liver of NAFLD models

To identify DEGs in each group, we used a fold change of $|\log FC| > 1$ and a FDR of $q = 0.05$ as the threshold. Numbers of DEGs detected were summarized in Fig. 2A and Table 2. Among DEX group, 704 genes were significantly differentially expressed (*P*.adj <0.05). Of those, 93 genes (13.2%) were significantly upregulated compared with genes in control group; 611 genes (86.8%) were downregulated. In the HSHF group, 403 genes were significantly differentially expressed. Of those, 341 genes (84.6%) were significantly upregulated compared with genes in control group; 62 genes (15.4%) were downregulated. In db/db group, 948 DEGs were detected. Of those, 589 genes (62.13%) were significantly upregulated; and up to 359 genes (37.9%) were downregulated (Fig. 2B).

We further analyzed the common DEGs between each of the two groups (Fig. 3 and Table 4). 91 DEGs were detected in both db/db mice and HSHF group, while 64 DEGs in both db/db mice with DEX group. However, only 24 DEGs were detected in both DEX group and HSHF group. The average ratio of overlapping DEGs between each mouse models ranged between 6% and 13%, suggesting the heterogeneity of these three NAFLD models (Fig. 3A–C). Of 91 common DEGs detected between HSHF and db/db mice, some of the genes are related to fatty acid transporter, lipoprotein transport and other lipid metabolic process (*Pparg*, *CD36*, *Apoa4*, *Elovl5*, *Abdcd1*) (Fig. 3A). Top genes related to lipid metabolism in each group were summarized in Table 3. Only 12 DEGs were detected in all three groups, with five up-regulated genes, which has been shown to be participated in lipid metabolism (*Apoa4*, *Thrsp*, *Sqle*) (Fig. 3D).

GO analysis

To further understand common and distinct pathways involved, GO tool was used to compare DEGs in all three groups. DEGs detected in each mouse model in GO analysis were classified into three groups, named as, cellular component, biological process and molecular function. Fig. 4A–C and Table S2 showed the top 20 pathways involved in each model. As shown in Fig. 4A–C, DEGs in three mouse models were mainly enriched in biological process. In db/db mice model, up-regulated DEGs were

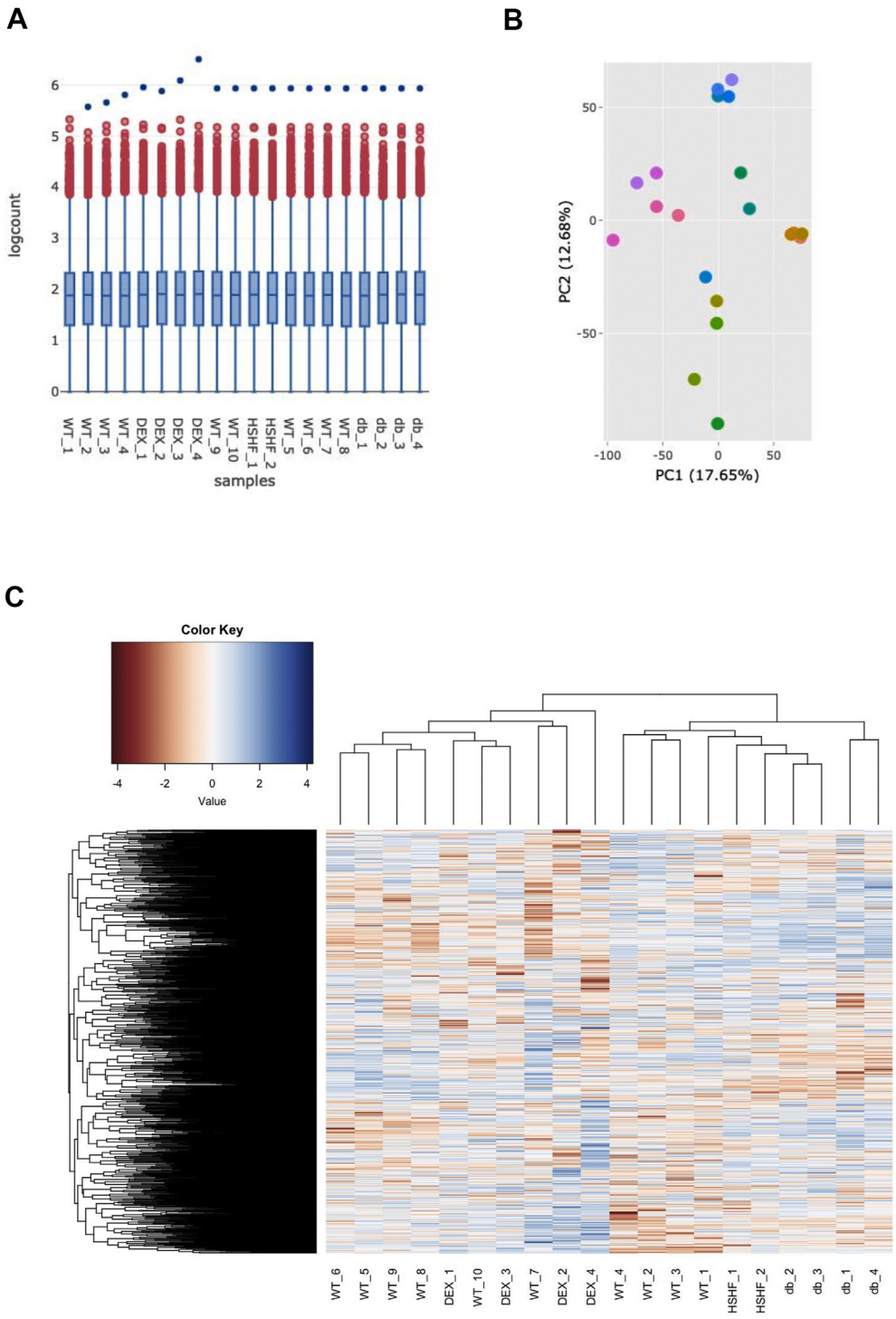

Figure 1 Gene expression patterns in the liver of three different mouse models of NAFLD by RNA-Seq analysis. **(A)** IQR boxplot and **(B)** PCA analysis shows normalized read counts in each mouse sample after batch-effect correction. **(C)** Heatmap shows expression patterns between different models after batch-effect correction.

mainly enriched in GO terms fatty acid metabolic process, xenobiotic metabolic process, sulfur compound metabolic process, and lipid catabolic process (Fig. 4A). In HSHF group, up-regulated DEGs were mainly enriched in GO terms leukocyte migration, positive regulation of lipid metabolic process, collagen metabolic process, and antigen processing and presentation of exogenous peptide antigen (Fig. 4B). In DEX group, however, most of the DEGs were down-regulated, which were mainly enriched in GO terms fatty acid metabolic process, steroid metabolic process, cellular ketone metabolic process and regulation of small molecule metabolic process (Fig. 4C).

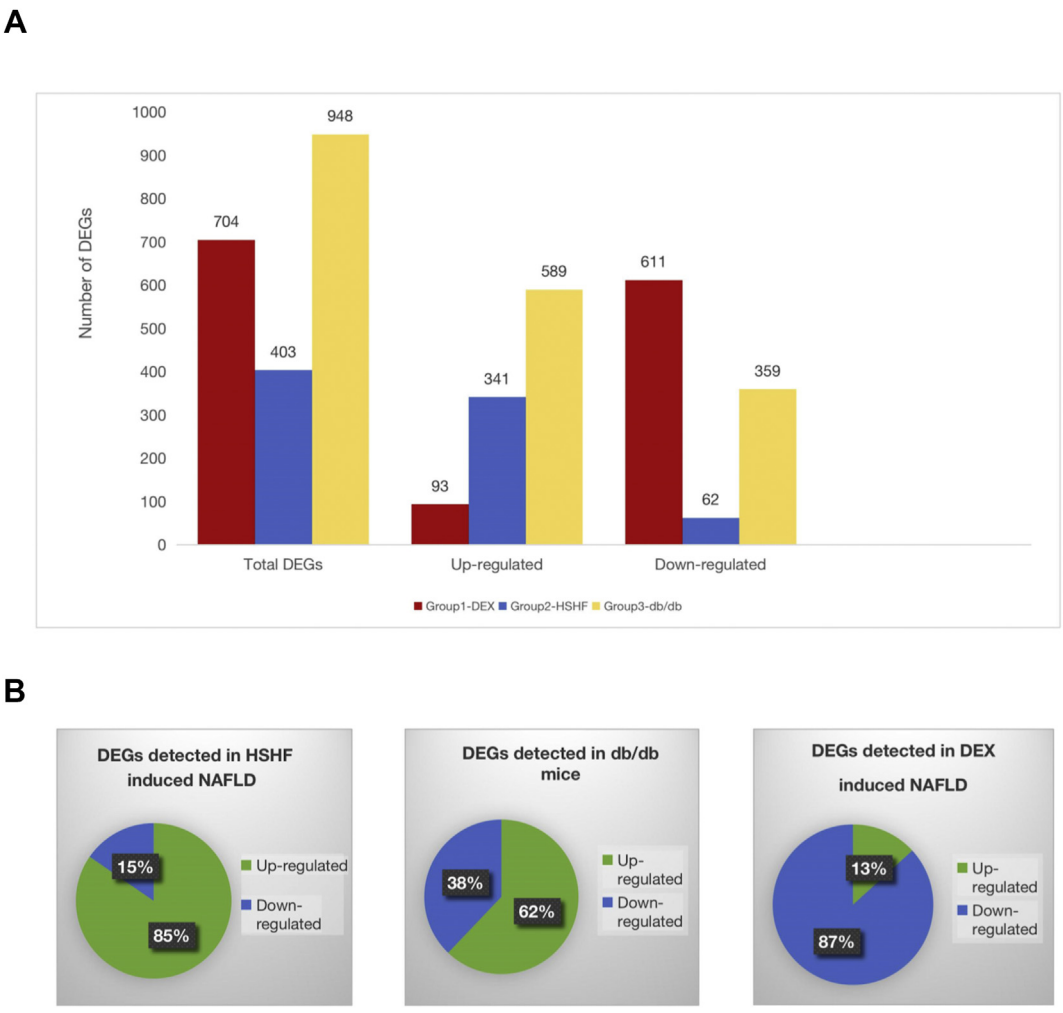

Figure 2 Analysis of differentially expressed genes (DEGs) in the liver of three different mouse models of NAFLD. **(A)** Distribution of up-regulated and down-regulated DEGs detected in each model. **(B)** Quantification of DEGs in three models. Bar graph shows the number of up-regulated (green color) and down-regulated genes (blue color) in each group compared with control group.

KEGG signaling enrichment analysis

KEGG signaling enrichment analysis was performed to investigate the pathways based on DEGs identified as well. Table S3 show the top 20 pathways involved in each cohort. In DEX group, down-regulated DEGs were mainly mapped to retinol metabolism, bile secretion, chemical carcinogenesis, and steroid hormone biosynthesis. In HSHF group, up-regulated DEGs were mainly overrepresented in PPAR signaling pathway, cholesterol metabolism, and biosynthesis of unsaturated fatty acid; while down-regulated DEGs were mainly mapped to steroid hormone biosynthesis, retinol metabolism, steroid biosynthesis, and chemical carcinogenesis. In db/db group, up-regulated DEGs were mainly

Table 2 Global similarity of three NAFLD models using adjusted significance thresholds.

Species	All DEGs	DEX	HSHF	*db/db*	Species
DEX	704		14	5	DEX
HSHF	403	24		17	HSHF
db/db	948	64	121		*db/db*

Overview of the pair-wise comparison of the transcriptomic analysis of NAFLD models on a single gene (lower triangle of the table, in grey) and pathway-level (upper triangle, in white). The column "regulated genes" provides the total number of differentially expressed genes for murine phenotype at a genome-wide.

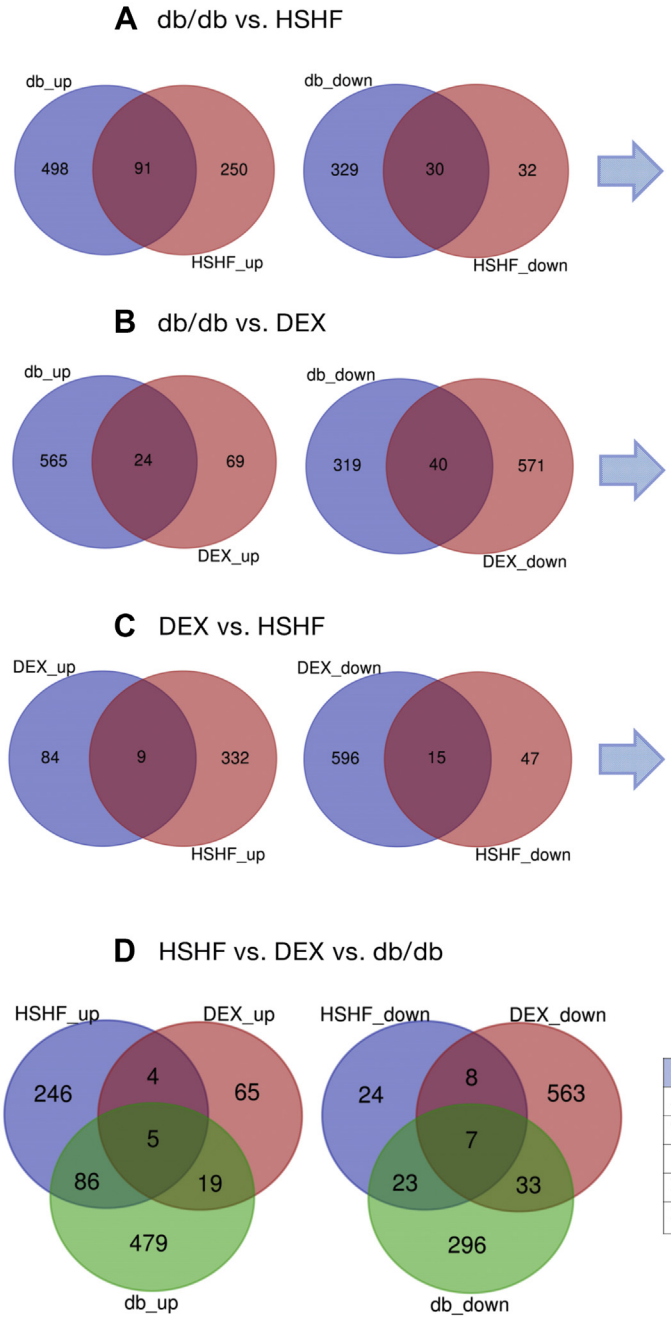

Selected DEGs	db/db	HSHF
PPARg	up	up
ELOVL5	up	up
APOA4	up	up
CD36	up	up
ABCD1	up	up
GSTA1	up	up
THRSP	up	up
CYP17A1	up	up
UNC119	up	up
CYP1A2	down	down
IGFBP1	down	down

Selected DEGs	db/db	DEX
INSIG2	up	up
SLC45A3	up	up
APOA4	up	up
THRSP	up	up
ACACB	up	up
ACOT1	up	up
MFSD2A	up	up
ELOVL2	down	down
SQLE	down	down
CYP51	down	down

Selected DEGs	DEX	HSHF
APOA4	up	up
THRSP	up	up
SQLE	down	down
IDI1	down	down
NSDHL	down	down
CYP51	down	down
UGT2B38/37	down	down
CYP2C54	down	down
HSD17B6	down	down

Selected DEGs	DEX	HSHF	db/db
APOA4	up	up	up
THRSP	up	up	up
SQLE	down	down	down
IDI1	down	down	down
HSD17B6	down	down	down

Figure 3 Common key DEGs detected in three different mouse models of NAFLD. **(A)** Common up- and down-regulated genes detected between db/db and HSHF group. **(B)** Common up- and down-regulated genes detected between db/db and DEX group. **(C)** Common up- and down-regulated genes detected between DEX and HSHF group. **(D)** Common DEGs detected in three NAFLD groups.

mapped to fatty acid metabolic process, sulfur compound metabolic process, nucleoside bisphosphate metabolic process and ribonucleoside bisphosphate metabolic process.

Comprehensive analysis of distinct and similar pathways in three different mouse models of NAFLD

Since comparing DEGs between different murine groups might overlook common biological pathways, we further clustered GO and KEGG pathways detected in three models. Clustering heatmap showed that three models displayed distinct pathway pattern (Fig. 5D and Table 5). Metabolic pathways, fatty acid degradation, fatty acid elongation, histidine metabolism, glycerolipid metabolism, glutathione metabolism, pyruvate metabolism and other pathways related to metabolism were distinctively enriched in db/db group. DEX group displayed distinct metabolic pathways as well, including cellular ketone metabolic process, lipid catabolic process, triglyceride biosynthesis process, neutral

Table 3 Key DEGs significantly changed involved in lipid metabolic process in the liver of each mouse model.

Metabolic process	Changes of top genes in each group								
	DEX induced NAFLD			HSHF induced NAFLD			*db/db*		
	Gene name	Log_2 (Fold Change)	FDR	Gene name	Log_2 (Fold Change)	FDR	Gene name	Log_2 (Fold Change)	FDR
Lipid	*Srebf1*	−2.28955	0.00116535	*Apoa4*	3.95879	0.00256724	*Pnpla3*	4.94022	0.00057796
	Elovl2	−1.01537	0.0011653	*Scd1*	2.75418	0.00256724	*Scd1*	3.04407	0.0005776
	Acnat1	−1.01528	0.019002	*Srebf1*	2.15722	0.00256724	*Elovl6*	3.11782	0.00057796
	Sqle	−1.97855	0.00116535	*Elovl5*	1.89249	0.00256724	*Elovl5*	2.46632	0.00057796
	Plin5	2.37117	0.00116535	*Lpl*	1.94893	0.00256724	*Cd36*	4.45396	0.0005779
	Acly	−1.65391	0.00116535	*Smpd3*	2.88631	0.0203045	*Pparg*	2.28283	0.00057796
	Insig1	−2.18166	0.00116535	*Cd36*	1.79329	0.00256724	*Ppargc1a*	2.11752	0.03424480
	Insig2	1.96634	0.0011653	*Pparg*	1.65057	0.00256724	*Acly*	1.45867	0.00057796
	Fasn	−1.68574	0.00298341	*Apoc2*	1.41882	0.0104423	*Acnat2*	4.83398	0.0005779
	Apoa4	3.01287	0.00116535	*Cyp17a1*	1.42665	0.00256724	*Insig2*	2.36451	0.00057796
	Fabp1	−1.0047	0.00116535				*Fasn*	2.07406	0.000577962
	Acot1	1.32154	0.0170247				*Apoa4*	1.6458	0.00057796
	Lpin1	1.99705	0.00116535				*Scd2*	1.66453	0.00057796
	Dhcr7	−1.36218	0.00116535				*Pck2*	−1.86523	0.00057796
	Hmgcr	−1.51934	0.00116535				*Hacl1*	1.3138	0.00155599
	Pcsk9	−2.11944	0.00116535				*Pdk4*	3.26674	0.00057796
	Acsl3	−2.48382	0.0011653				*Gpam*	2.4615	0.00057796
	Acox1	−1.09071	0.0052477				*Pdk1*	1.47899	0.00057796
	Fads2	−1.20849	0.00116535				*Gpat2*	−1.23393	0.02466420
	Fads3	−1.71553	0.00116535				*Fabp5*	−1.53929	0.000577962
	Soat2	−1.00581	0.00593422				*Fabp4*	1.10654	0.00057796
							Acot1	1.70572	0.00057796
	Lpin1	−2.43886	0.00057796						
	Elovl2	−1.84094	0.00057796						
	Acsl5	1.03864	0.00057796						

lipid biosynthesis process, acylglycerol biosynthesis process, as well as cofactor biosynthesis process. In HSHF group, distinct pathways detected mainly focus on cholesterol biosynthetic process, cholesterol mechanism, fat digestion and absorption, and steroid biosynthesis process. Also, HSHF group showed specific changes in immune related metabolic pathways, such as cytokine—cytokine receptor interaction, positive regulation of adaptive immune response, and leukocyte activation involved in inflammatory response.

Venn diagram showed common pathways detected between each group (Fig. 5A—C). Among all three groups, HSHF group and db/db group displayed most shared pathways based on DEGs detected (Fig. 5A). Interestingly, up to 34 common pathways were detected between db/db group and DEX group even with very few common DEGs detected. Total numbers of GO and KEGG pathways detected in each model were summarized in Table 2. To further understand common pathways detected among all three groups, we clustered resulted from GO and KEGG analysis (Fig. 6). With red dot representing down-regulated pathways and blue representing up-regulated pathways, we could easily recognize different patterns of pathways enriched in three groups. Pathway analysis revealed that steroid metabolic process and regulation of small molecule metabolic pathway were common pathways detected in all three groups. Even though common pathways were detected between DEX group with either db/db or HSHF group, most pathways show opposite regulation status.

Discussion

NAFLD is a continuous spectrum of diseases characterized by excessive lipid accumulation in hepatocytes.[3] NAFLD progresses from simple liver steatosis to non-alcoholic steatohepatitis and, in more severe cases, to liver fibrosis, cirrhosis, and hepatocellular carcinoma (HCC).[3] Since mouse models are the cornerstone for mechanistic and interventional studies of disease pathogenesis, many animal models of NAFLD have already been developed.[15,16] In this study, we analyzed three different murine models to evaluate differences in gene expression and pathways between them. We chose commonly used HSHF diet as diet-induced NALFD model, genetic obese db/db mice and DEX treated mouse model as drug-induced model. Through comprehensive analysis from transcriptome data, we mapped DEGs detected in all three groups to GO and KEGG database, and further compared

Table 4 Common key DEGs in each moue model of NAFLD in comparison with each other.

Types of DEGs	Gene Names
HSHF *vs*. *db/db*	
DEGs upregulated in both HSHF induced NAFLD and *db/db* mice ($n = 91$)	*Ly6d*, *Cyp2a22*, *Themis*, *Ttc39a*, *Acnat2*, *Acss3*, *Hamp2*, *Cd36*, *Rcan2*, *Lcn2*, *Cidec*, *Cyp17a1*, *Extl1*, *Osbpl3*, *Robo1*, *Tmem28*, *Smpd3*, *Eda*, *Fam131c*, *Scd1*, *Tubb2a*, *Ubd*, *Gal3st1*, *Slc35f2*, *Elovl5*, *Tceal8*, *Tmem98*, *Abcb1a*, *Dntt*, *Pparg*, *Saa2*, *2010003K11Rik*, *Sulf2*, *Mest*, *Acot11*, *Vnn1*, *Fam83f*, *S100a10*, *Lgalsl*, *Chchd6*, *Limk1*, *Mmd2*, *Thrsp*, *Gdf15*, *Anxa2*, *Aqp8*, *Cyp2a4*, *Them6*, *Tenm3*, *Slc17a4*, *Scd2*, *Apoa4*, *Rxrg*, *Fam124a*, *Mms22l*, *Bhlhb9*, *Acyp2*, *Acaa1b*, *Tnfrsf19*, *Mup19*, *Ifi27l2b*, *Saa1*, *Enc1*, *Myo1d*, *Ptp4a3*, *Anxa5*, *Copz2*, *Mgst3*, *S100a11*, *Sorbs1*, *Cldn2*, *Synj2*, *Lgals1*, *Adam11*, *Gsta1*,*Abcd1*, *Ppm1h*, *Mcm5*, *Wfdc2*, *Gale*, *Srxn1*, *Ermp1*, *Abcd2*, *Samd9l*, *Fabp4*, *Serpina7*, *Unc119*, *Pgd*, *Tnip1*, *Maged2*, *Gas6*
DEGs downregulated in both HSHF induced NAFLD and *db/db* mice ($n = 30$)	*Slc13a2*, *Cyp1a2*, *Gadd45g*, *Ppp1r3g*, *Mup13*, *BC089597*, *Igfbp1*, *Fam222a*, *Cyp51*, *Sqle*, *Mup15*, *C8b*, *Hsd17b6*, *Mup14*, *Idi1*, *Lama3*, *Cxcl13*, *Lifr*, *Susd4*, *E130012A19Rik*, *Cabyr*, *Mup11*, *Cyp7b1*, *Mup12*, *Cadm4*, *Selenbp2*, *Gpr110*, *Mup7*, *Enho*, *Serpina1e*
DEGs upregulated in HSHF induced NAFLD but downregulated in *db/db* mice ($n = 15$)	*Pld4*, *Lsp1*, *H2-Eb1*, *Dsg1c*, *Smoc2*, *Nrep*, *Arhgdib*, *Tnfsf12*, *Selplg*, *Coro1a*, *Ccl6*, *H2-Ab1*, *H2-Aa*, *H2-DMb1*, *Tlr12*
DEGs upregulated in *db/db* but downregulated in HSHF induced NAFLD mice ($n = 8$)	*Acot6*, *Raet1d*, *Raet1e*, *Cyp2c40*, *Etnppl*, *Dct*, *G6pc*, *Cyp26a1*
HSHF *vs*. DEX	
DEGs upregulated in both HSHF induced NAFLD and DEX-treated mice ($n = 9$)	*Apoa4*, *Lcn2*, *Saa1*, *Gramd1b*, *Gdf15*, *Thrsp*, *Lyve1*, *Rgs16*, *Plin3*
DEGs downregulated in both HSHF induced NAFLD and DEX-treated mice ($n = 15$)	*Cyp51*, *Fbf1*, *Sqle*, *Sik1*, *Cabyr*, *Hsd17b6*, *Nsdhl*, *Sc4mol*, *Ccbl2*, *Lifr*, *Ugt2b37*, *Idi1*, *Ugt2b38*, *Cyp2c54*, *BC089597*
DEGs upregulated in HSHF induced NAFLD but downregulated in DEX-treated mice ($n = 24$)	*Aqp8*, *Srebf1*, *Serpina7*, *H2-Ab1*, *Hamp2*, *H2-Aa*, *Cd74*, *Tmem106a*, *Nrep*, *Mpeg1*, *Krt18*, *Cldn2*, *Abcg5*, *Paqr7*, *Trp53i11*, *Abcd1*, *Acaa1b*, *Tenm3*, *Ddx58*, *Fads2*, *Abcg8*, *Sorbs1*, *Klhdc7a*, *Cybb*
DEGs upregulated in DEX-treated but downregulated in HSHF induced NAFLD mice ($n = 5$)	*Tat*, *Arrdc2*, *Igfbp1*, *Gadd45g*, *Scara5*
DEX *vs*. *db/db*	
DEGs upregulated in both DEX-treated and *db/db* mice ($n = 24$)	*Acacb*, *Acot1*, *Treh*, *Mt2*, *Obp2a*, *Agpat9*, *Cyp2b10*, *Lcn2*, *Mt1*, *Ppp1r3c*, *Gdf15*, *Apoa4*, *Saa1 Slc45a3*, *Cyp4a14*, *Prob1*, *Insig2*, *Chd1l*, *Mfsd2a*, *Fmo5*, *Thrsp*, *Gldc*, *1810011O10Rik*, *Bhmt*
DEGs downregulated in both DEX-treated and *db/db* mice ($n = 40$)	*Zfp707*, *Marco*, *Ccnd1*, *Dna2*, *Irgm2*, *Rapgef4*, *Cyp51*, *Lifr*, *Dbp*, *Ttc39c*, *Apol9b*, *H2-Aa*, *Mup3*, *Irf6*, *Elovl2*, *Mug2*, *BC089597*, *Fbxo21*, *Cdh1*, *Slco1a1*, *Hsd17b6*, *Rnase4*, *Sel1l3*, *Adh6-ps1*, *Ces1c*, *Phlda1*, *Keg1*, *Ces1b*, *Nrp1*, *Nudt7*, *Sqle*, *H2-Ab1*, *Idi1*, *Mapk15*, *Sort1*, *Cabyr*, *Aox3*, *Marveld2*, *Cyp2u1*, *Nrep*
DEGs upregulated in DEX-treated but downregulated in *db/db* mice ($n = 6$)	*Porcn*, *Serpine2*, *Lipin1*, *Gadd45g*, *Igfbp1*, *AA986860*
DEGs downregulated in DEX-treated but upregulated in *db/db* mice ($n = 42$)	*Ccng1*, *Hnmt*, *Gtdc1*, *5033411D12Rik*, *Caln1*, *Tenm3*, *Gm13152*, *Acad10*, *Hacl1*, *Abcd1*, *Rtn4*, *Hamp2*, *Cd59a*, *Btbd7*, *Adra1b*, *Pls3*, *Entpd5*, *Tlr5*, *Rwdd3*, *E2f3*, *Sorbs1*, *Pla2g15*, *Fasn*, *Nat8*, *Slc25a10*, *Aldh1a1*, *Bche*, *Paqr9*, *Ebpl*, *Rdh16*, *Prkdc*, *Slc16a7*, *Aqp8*, *Nfe2l2*, *Acly*, *Lrit1*, *Cyp2c38*, *Acaa1b*, *Serpina7*, *Mme*, *Prlr*, *Cldn2*
DEX *vs*. HSHF *vs*. *db/db*	
DEGs upregulated in all three groups ($n = 5$)	*Apoa4*, *Lcn2*, *Saa1*, *Gdf15*, *Thrsp*
DEGs downregulated in all three groups ($n = 7$)	*Cyp51*, *Sqle*, *Cabyr*, *Hsd17b6*, *Lifr*, *Idi1*, *BC089597*
DEGs upregulated in DEX-treated but downregulated in both *db/db* and HSHF induced NAFLD mice ($n = 2$)	*Gadd45g*, *Igfbp1*
DEGs downregulated in DEX-treated but upregulated in both *db/db* and HSHF induced NAFLD mice ($n = 8$)	*Tenm3*, *Abcd1*, *Hamp2*, *Sorbs1*, *Aqp8*, *Acaa1b*, *Serpina7*, *Cldn2*
DEGs upregulated in HSHF-induced NAFLD but upregulated in both *db/db* and DEX-treated mice ($n = 3$)	*H2-Ab1*, *H2-Aa*, *Nrep*

DEGs and pathways in each group with each other. Only 12 DEGs were detected in all three groups, five of them were up-regulated genes including *Apoa4*, *Thrsp*, which are known to participate in lipid metabolism. Pathway analysis revealed that metabolic pathways, steroid metabolic process, regulation of small molecule metabolic pathway were common biological functions in all three groups. We further compared results from pathway analysis in a more specific way, and detected a more similar regulation pattern of metabolic pathways between HSHF and db/db group compared to DEX group. Overall, our clustering analysis showed a more similar gene expression pattern between db/db mice with HSHF group.

As known to all already, most commonly used methods to generate NAFLD models are western diet models.[15] Western-diet is a diet high in saturated fat, trans-fat, and sugar. In humans, this type of diet has been shown to induce obesity, metabolic syndrome, NAFLD, and potentially, NASH.[17] In the liver of mice fed with a high-fat diet (HFD), exaggerated free fatty acid levels were detected, inducing hepatic insulin resistance, decreased fatty acid oxidation, and increased *de novo* lipogenesis in hepatocytes.[18] HSHF diet, however, is a combination of both HFD and high fructose diet. Findings obtained with C57BL/6 mice fed HSHF diet suggested that fructose consumption is necessary for the progression of fat deposition to fibrogenesis in liver.[19,20] Though weight gain, body fat and liver steatosis were both detected in HFD and HSHF mouse models, hepatic oxidative stress, liver macrophage numbers, fibrogenesis and collagen deposition were only detected to be increased in mice fed the HSHF diet, suggesting altered immune signaling pathway involved apart from lipid metabolism change in the liver of HSHF diet induced NAFLD model.[21,22] Genetic modified db/db mice are homozygous for the autosomal recessive diabetic gene (db). The db gene encodes a point mutation of the leptin receptor (Ob-Rb), which leads to defective leptin signalling. These mice have persistent hyperphagia, are obese and diabetic, and develop hepatic steatosis.[7] db/db mice do not spontaneously develop inflammation when fed a normal control diet.[7] So, when fed a standard diet without additional hits, these mice are useful models of NAFLD. Glucocorticoids, one of the most used classes of corticosteroids used in everyday clinic, are commonly used at high doses and for prolonged periods in the treatment of a variety of diseases. Among the many side effects of glucocorticoids, most known related to metabolism are increased insulin resistance with disturbances in glucose homeostasis and increased deposition of lipids in the liver, mostly triglycerides.[23,24,25] Since different murine models of NAFLD focus on different aspect of the disease pathology, the pathway analysis may provide in itself additional insights.

In defining molecular mechanisms of obesity-associated NAFLD, it has been well-established that steatosis occurs when the rate of fatty acid synthesis is greater than the rate of fatty acid oxidation and secretion.[2] For instance, our recent studies showed that upregulation of lipogenic genes or defects in the fatty acid oxidation could induce liver steatosis and contribute to fatty liver.[26,27] However, lipogenic genes were repressed by GC-GR signaling in the liver,[28] suggesting that GCs-induced hepatosteatosis could be attributed to alternative mechanisms.[29] Indeed, recent studies showed that excess glucocorticoids could promote hepatic lipid deposition through enhancing fatty acid uptake in the liver and repressing fatty acid oxidation.[29] Together, these reports suggest that the molecular mechanisms of different NAFLD models might be distinct, which needs further intensive studies. In the present study, we provided a comprehensive transcriptome analysis of liver tissue between three totally different mouse models of NAFLD. We detected very few common genes related to metabolism in all three models, including *Apoa4*, *Thrsp* and *Sqle*. Apoa4, apolipoprotein A-IV (ApoA-IV), has been well known for its role in lipid metabolism and metabolic regulation *in vitro* and *in vivo*.[30] Previous studies have already indicated that high fat diet, steatosis or dexamehasone treatment could increase Apoa4 expression level in the liver.[31] Besides, hepatic ApoA-IV expression could serve as an early diagnostic biomarker in liver fibrosis.[32] Thrsp, known as a nuclear protein in the regulation of lipid metabolism, has been reported to be highly expressed in the liver and adipose tissue.[33] Sqle, also known as squelene monooxygenase, a key rate-enzyme in cholesterol biosynthesis, has been revealed as a top outlier metabolic gene overexpressed in NAFLD-induced hepatocellular carcinoma.[34]

Results from GO and KEGG pathway analysis among three groups showed very few common pathways. We used clustering heatmap and dot map to show that three mouse models displayed distinct pathway pattern. Apart from the expected enrichment of gene sets associated with lipid metabolism confirming changes in fatty acid biology, an enrichment of several gene sets associated with inflammation was observed in HSHF group mainly. As previously reported in other study, inflammation response pathways in NAFLD might be considered as one of the major relevance and may already be active on a subcellular level, even without yet visible change on a cellular or morphological level.[35,36] This subcellular change might explain the underlying mechanism of prolonged HSHF diet induced NAFLD development and possibly progression to NASH.[37,38] As for DEX induced NAFLD, previous studies already showed that pathways of lipid deposition stimulated by excess glucocorticoids include stimulation of *de novo* lipogenesis, increased release of free fatty acids from adipose stores and stimulation of their uptake by the liver, etc.[39,40] In our pathway analysis, we found DEX up-regulates triglyceride metabolic process, neutral lipid biosynthesis, as well as other lipid metabolic process, while down-regulates fatty acid metabolic process and steroid metabolic process. Thus, our study provided information of gene transcription changes in the liver of different NAFLD models, indicating very few common pathways cross different models.

Several limitations should be pointed out in our study. Firstly, the number size is relatively small. Secondly, we used only pathway analysis, which may possibly overlook certain similarities between different models. Thirdly, our present study is a descriptive study, functional experiments

A

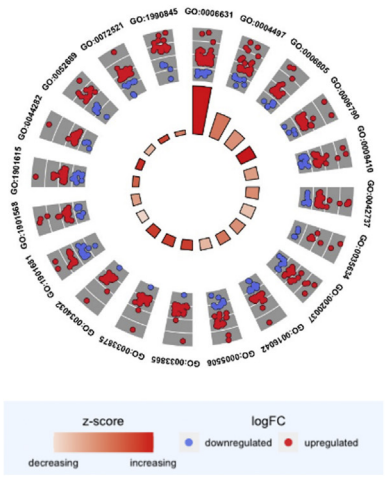

ID	Term	Category	Counts	adj.p value
GO:0006631	Fatty acid metabolic process	BP	70	1.79824E-25
GO:0004497	Monooxygenase activity	MF	34	4.34952E-15
GO:0006805	Xenobiotic metabolic process	BP	27	9.77865E-12
GO:0006790	Sulfur compound metabolic process	BP	41	3.3873E-11
GO:0009410	Response to xenobiotic stimulus	BP	35	1.44137E-09
GO:0042737	Drug catabolic process	BP	28	1.46838E-09
GO:0035634	Response to stilbenoid	BP	12	1.56246E-09
GO:0020037	Heme binding	MF	27	4.92808E-09
GO:0016042	Lipid catabolic process	BP	39	9.97764E-09
GO:0005506	Iron ion binding	MF	27	1.46698E-08
GO:0033865	Nucleoside bisphosphate metabolic process	BP	21	2.63747E-08
GO:0033875	Ribonucleoside bisphosphate metabolic process	BP	21	2.63747E-08
GO:0034032	Purine nucleoside bisphosphate metabolic process	BP	21	2.63747E-08
GO:1901681	Sulfur compound binding	MF	32	1.56536E-07
GO:1901568	Fatty acid derivative metabolic process	BP	23	1.67905E-07
GO:0006732	Coenzyme metabolic process	BP	37	6.01355E-07
GO:1901615	Organic hydroxy compound metabolic process	BP	46	1.0773E-06
GO:0044282	Small molecule catabolic process	BP	35	1.08133E-06
GO:0052689	Carboxylic ester hydrolase activity	BP	23	1.81589E-06
GO:0072521	Purine-containing compound metabolic process	BP	45	4.3059E-06

B

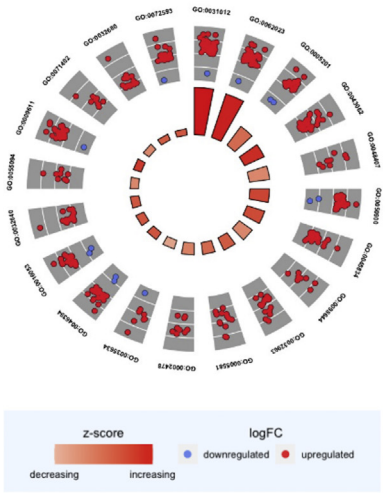

ID	Term	Category	Counts	adj.p value
GO:0031012	Extracellular matrix	CC	43	6.11848E-17
GO:0062023	Collagen-containing extracellular matrix	CC	37	1.63108E-16
GO:0005201	Extracellular matrix structural constituent	CC	20	1.15877E-10
GO:0043062	Extracellular structure organization	CC	29	3.45171E-10
GO:0048407	Platelet-derived growth factor binding	BP	8	7.23933E-10
GO:0050900	Leukocyte migration	BP	29	1.20114E-09
GO:0045834	Positive regulation of lipid metabolic process	BP	20	2.28904E-09
GO:0098644	Complex of collagen trimers	CC	8	8.28019E-09
GO:0032963	Collagen metabolic process	BP	16	2.6586E-08
GO:0005581	Collagen trimer	CC	13	8.22288E-08
GO:0002478	Antigen processing and presentation of exogenous peptide antigen	BP	9	8.91249E-08
GO:0035634	Response to stilbenoid	BP	8	4.44102E-07
GO:0046394	Carboxylic acid biosynthetic process	BP	25	5.93085E-07
GO:0016053	Organic acid biosynthetic process	BP	25	5.93085E-07
GO:0032640	Tumor necrosis factor production	BP	17	6.15809E-07
GO:0055094	Response to lipoprotein particle	BP	8	8.08701E-07
GO:0009611	Response to wounding	BP	29	8.08701E-07
GO:0071402	Cellular response to lipoprotein particle stimulus	BP	8	1.434E-06
GO:0032680	Regulation of tumor necrosis factor production	BP	16	2.30663E-06
GO:0072593	Reactive oxygen species metabolic process	BP	21	2.30744E-06

C

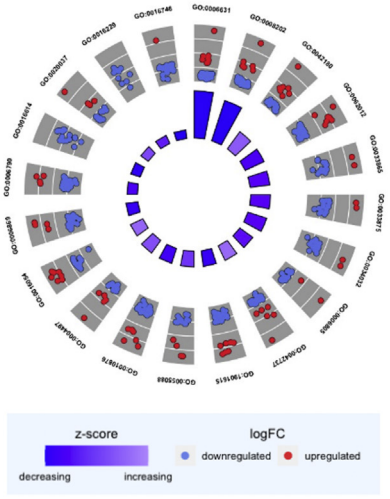

ID	Term	Category	Counts	adj.p value
GO:0006631	Fatty acid metabolic process	BP	49	2.31373E-15
GO:0008202	Steroid metabolic process	BP	42	3.33445E-14
GO:0042180	Cellular ketone metabolic process	BP	27	5.68867E-09
GO:0062012	Regulation of small molecule metabolic process	BP	37	6.7793E-09
GO:0033865	Nucleoside bisphosphate metabolic process	BP	19	1.25691E-08
GO:0033875	Ribonucleoside bisphosphate metabolic process	BP	19	1.25691E-08
GO:0034032	Purine nucleoside bisphosphate metabolic process	BP	19	1.25691E-08
GO:0006805	Xenobiotic metabolic process	BP	19	9.72529E-08
GO:0042737	Drug catabolic process	BP	22	9.72529E-08
GO:1901615	Organic hydroxy compound metabolic process	BP	41	1.13469E-07
GO:0055088	Lipid homeostasis	MF	21	1.21897E-07
GO:0010876	Lipid localization	MF	35	1.21897E-07
GO:0004497	Monooxygenase activity	MF	22	1.28147E-07
GO:0016054	Organic acid catabolic process	BP	25	3.8076E-07
GO:0006869	Lipid transport	MF	31	1.02013E-06
GO:0006790	Sulfur compound metabolic process	BP	27	2.6078E-06
GO:0016614	Oxidoreductase activity, acting on ch-oh group of donors	MF	20	3.25966E-06
GO:0020037	Heme binding	MF	20	4.81466E-06
GO:0016229	Steroid dehydrogenase activity	MF	11	6.00167E-06
GO:0016746	Transferase activity, transferring acyl groups	MF	26	6.91856E-06

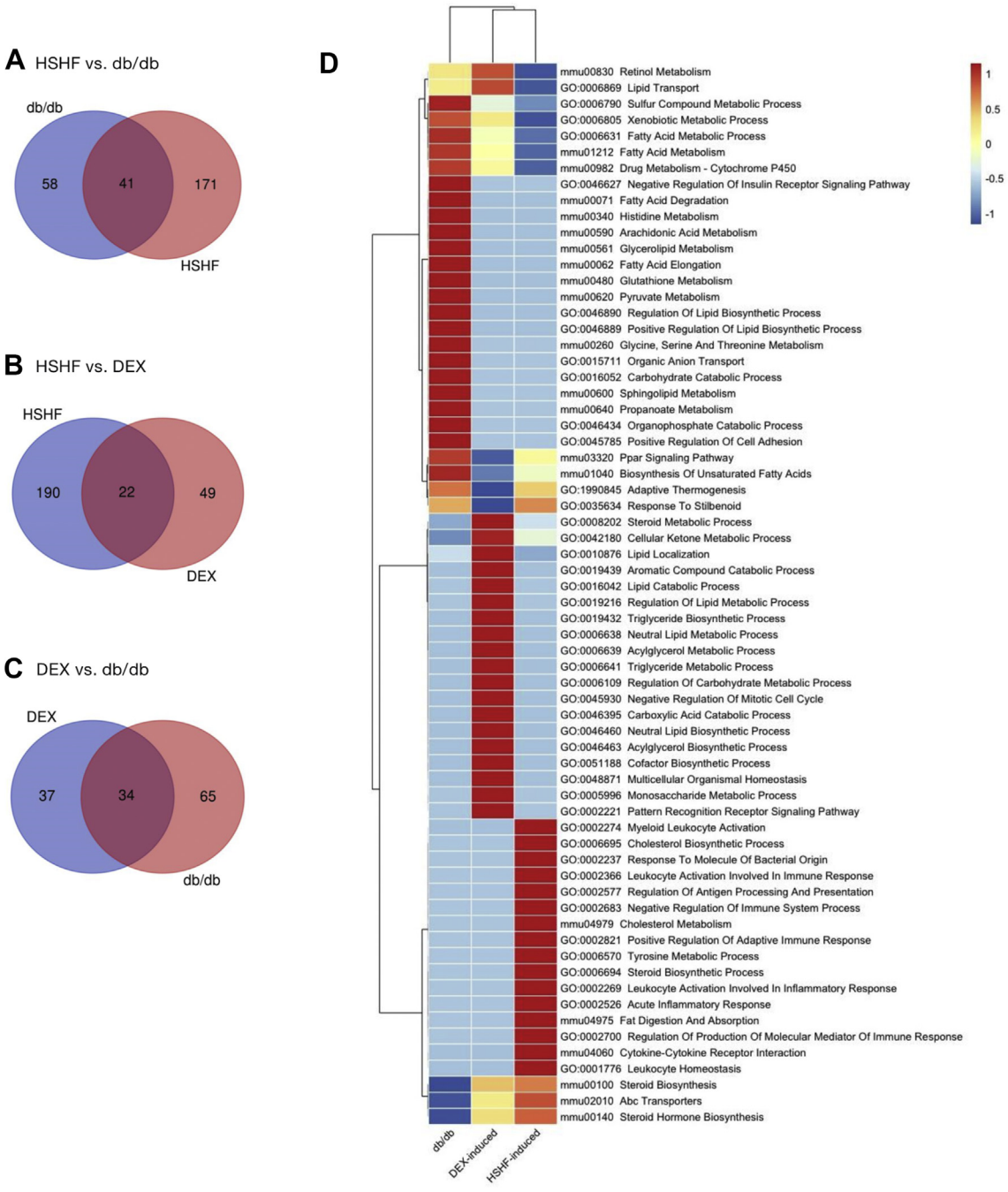

Figure 5 Comparison of over-presented functional enrichment analysis between three models performed on shared pathways. **(A)** Comparison of over-presented functional enrichment analysis between HSHF and db/db group. **(B)** Comparison of over-presented functional enrichment analysis between HSHF and DEX group. **(C)** Comparison of over-presented functional enrichment analysis between DEX and db/db group. **(D)** Selected functional enrichment analysis show distinct pattern in each group. Over-represented functions are shown in the heat map with adjusted P value < 0.05. Red color representing significantly changed pathway, blue color representing insignificant result.

Figure 4 Over-represented pathways of Gene Ontology (GO) analysis and significantly enriched GO terms of DEGs in different models of NAFLD. **(A)** Over represented pathways of Gene Ontology (GO) analysis and significantly enriched GO terms of DEGs in db/db mice; **(B)** Over represented pathways of Gene Ontology (GO) analysis and significantly enriched GO terms of DEGs in HSHF induced NAFLD mice; **(C)** Over represented pathways of Gene Ontology (GO) analysis and significantly enriched GO terms of DEGs in DEX treated mice.

Table 5 Comparison of over-presented functional enrichment analysis performed on the shared pathways between three mouse models of NAFLD.

Pathways	Different Models					
GO and KEGG pathway terms	DEX		HSHF		*db/db*	
	Regulation	BH.p value	Regulation	BH.p value	Regulation	BH.p value
GO:0008202 Steroid Metabolic Process	down	1.10783E-11	down	3.9539E-05	up	0.000592725
GO:0010876 Lipid Localization	down	1.20163E-05	up	7.07082E-05	up	5.54001E-05
GO:0006805 Xenobiotic Metabolic Process	down	6.87516E-07	down	0.015039461	up	4.63612E-09
GO:0062012 Regulation Of Small Molecule Metabolic Process	down	1.97349E-06	up	1.42514E-05	up	0.005334651
GO:0044282 Small Molecule Catabolic Process	up	0.003188734	up	0.006204059	up	4.63612E-09
GO:0035634 Response To Stilbenoid	down	0.00084057	up	1.76742E-06	up	2.68169E-06
GO:0042737 Drug Catabolic Process	up	0.003188734	down	0.02905059	up	9.41721E-08
GO:0062013 Positive Regulation Of Small Molecule Metabolic Process	down	0.006111985	up	4.26301E-06	up	0.003422671
GO:1901615 Organic Hydroxy Compound Metabolic Process	down	1.14533E-05	down	0.002631838	up	1.68246E-06
Mmu00980 Metabolism Of Xenobiotics By Cytochrome P450	down	0.00366925	down	0.04096318	up	0.007078388
mmu02010 ABC Transporters	down	0.005205567	up	0.00718615	up	0.013547692
mmu03320 PPAR signaling pathway	/	/	up	4.45039E-05	up	1.96799E-08
mmu01212 Fatty acid metabolism	down	0.020176687	/	/	up	0.000577213
mmu01040 Biosynthesis of unsaturated fatty acids	/	/	up	0.001703037	up	3.42971E-06
mmu00830 Retinol metabolism	down	1.44555E-11	down	9.7534E-08	up	2.35428E-10
mmu00591 Linoleic acid metabolism	/	/	down	0.019186006	up	0.049841292
mmu00100 Steroid biosynthesis	down	0.000107417	down	2.97813E-05	/	/
GO:1990845 Adaptive thermogenesis	/	/	up	9.50564E-05	up	1.467E-05
GO:1901568 Fatty acid derivative metabolic process	down	0.000479109	/	/	up	9.22256E-06
GO:0120162 Positive regulation of cold-induced thermogenesis	/	/	up	0.001272215	up	0.003804817
GO:0009410 Response to xenobiotic stimulus	down	0.000143497	/	/	up	9.50984E-07
GO:0006869 Lipid transport	down	1.37567E-05	/	/	up	0.000688304
GO:0006790 Sulfur compound metabolic process	down	5.15667E-05	/	/	up	6.22691E-15
GO:0006732 Coenzyme metabolic process	down	9.23777E-05	/	/	up	4.63612E-09
GO:0001659 Temperature homeostasis	/	/	up	7.54435E-05	up	0.003811025

GO, Gene Ontology; NAFLD, nonalcoholic fatty liver disease; HSHF, high sucrose high fat; BH, Benjamini and Hochberg.

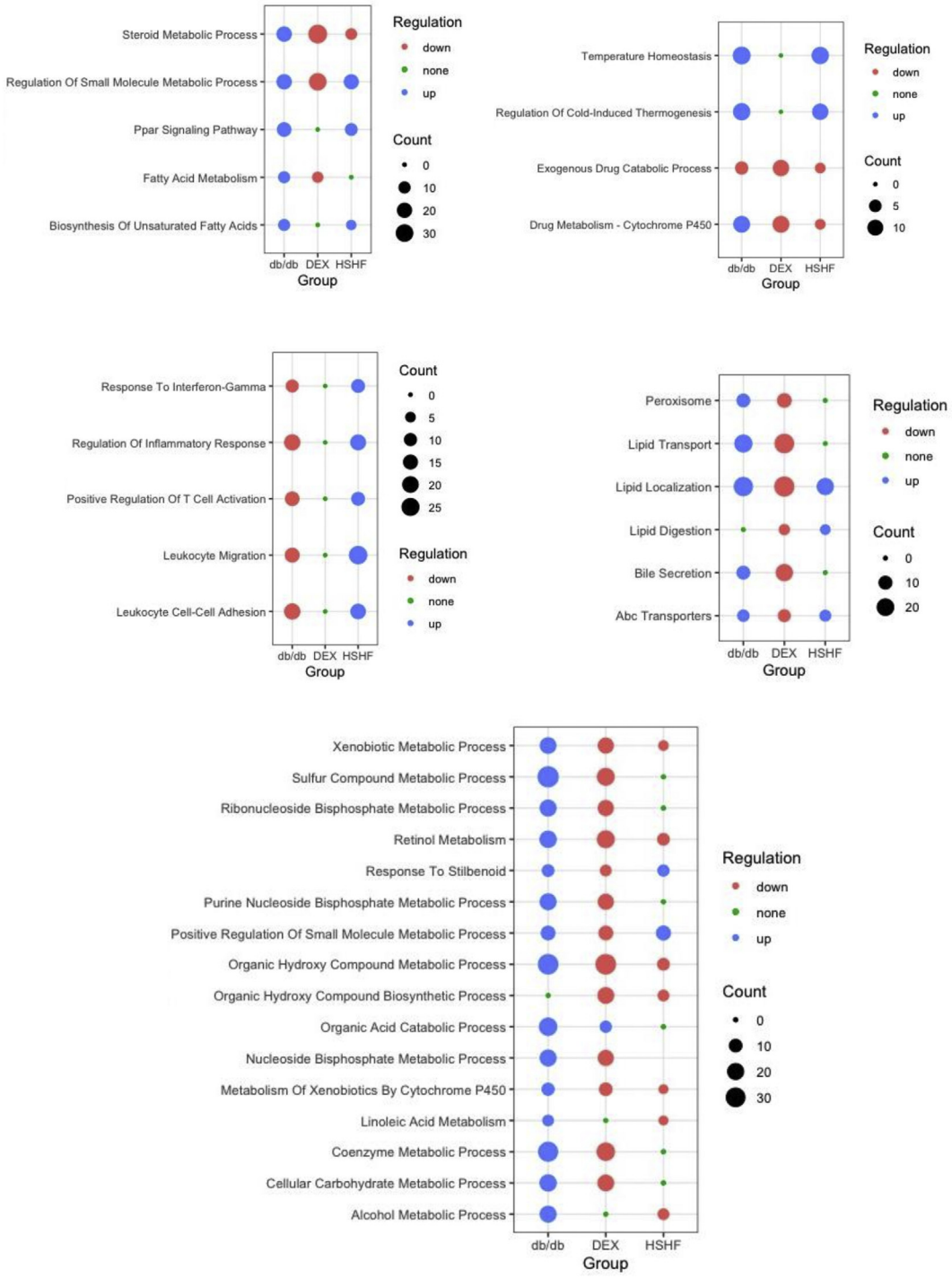

Figure 6 Functional enrichment pathway analysis show distinct regulation status of common pathways in three different mouse models of NAFLD.

should be performed to further explore the role and mechanisms of target genes in the development of fatty liver disease.

Conclusions

The present study reveals both transcriptional similarities and differences between three different NAFLD models. Our results suggest that NAFLD is a heterogeneous disease with highly variable molecular mechanisms.

Conflict of interests

The authors have no conflict of interests to declare.

Acknowledgements

This work was supported by National Key Research and Development Program of China (No. 2018YFA0800402), National Natural Science Foundation of China (No. 81974119), Shanghai Science Foundation (No. 18ZR1437800), and Shanghai Jiaotong University Foundation (No. shklab202012).

Appendix A. Supplementary data

Supplementary data to this article can be found online at https://doi.org/10.1016/j.gendis.2021.02.008.

References

1. Younossi Z, Anstee QM, Marietti M, et al. Global burden of NAFLD and NASH: trends, predictions, risk factors and prevention. *Nat Rev Gastroenterol Hepatol*. 2018;15(1):11—20.
2. Friedman SL, Neuschwander-Tetri BA, Rinella M, Sanyal AJ. Mechanisms of NAFLD development and therapeutic strategies. *Nat Med*. 2018;24(7):908—922.
3. Brunt EM. Pathology of nonalcoholic fatty liver disease. *Nat Rev Gastroenterol Hepatol*. 2010;7(4):195—203.
4. Asrih M, Jornayvaz FR. Diets and nonalcoholic fatty liver disease: the good and the bad. *Clin Nutr*. 2014;33(2):186—190.
5. de Wit NJW, Afman LA, Mensink M, Müller M. Phenotyping the effect of diet on non-alcoholic fatty liver disease. *J Hepatol*. 2012;57(6):1370—1373.
6. Trak-Smayra V, Paradis V, Massart J, Nasser S, Jebara V, Fromenty B. Pathology of the liver in obese and diabetic ob/ob and db/db mice fed a standard or high-calorie diet. *Int J Exp Pathol*. 2011;92(6):413—421.
7. Anstee QM, Goldin RD. Mouse models in non-alcoholic fatty liver disease and steatohepatitis research. *Int J Exp Pathol*. 2006;87(1):1—16.
8. Woods CP, Hazlehurst JM, Tomlinson JW. Glucocorticoids and non-alcoholic fatty liver disease. *J Steroid Biochem Mol Biol*. 2015;154:94—103.
9. Wang Z, Gerstein M, Snyder M. RNA-Seq: a revolutionary tool for transcriptomics. *Nat Rev Genet*. 2009;10(1):57—63.
10. Kukurba KR, Montgomery SB. RNA sequencing and analysis. *Cold Spring Harb Protoc*. 2015;2015(11):951—969.
11. Feng G, Li XP, Niu CY, et al. Bioinformatics analysis reveals novel core genes associated with nonalcoholic fatty liver disease and nonalcoholic steatohepatitis. *Gene*. 2020;742:144549.
12. Huang S, Sun C, Hou Y, et al. A comprehensive bioinformatics analysis on multiple Gene Expression Omnibus datasets of nonalcoholic fatty liver disease and nonalcoholic steatohepatitis. *Sci Rep*. 2018;8(1):7630.
13. Banasik K, Justesen JM, Hornbak M, et al. Bioinformatics-driven identification and examination of candidate genes for non-alcoholic fatty liver disease. *PloS One*. 2011;6(1):e16542.
14. Ishimoto T, Lanaspa MA, Rivard CJ, et al. High-fat and high--sucrose (western) diet induces steatohepatitis that is dependent on fructokinase. *Hepatology*. 2013;58(5):1632—1643.
15. Lau JKC, Zhang X, Yu J. Animal models of non-alcoholic fatty liver disease: current perspectives and recent advances. *J Pathol*. 2017;241(1):36—44.
16. Stephenson K, Kennedy L, Hargrove L, et al. Updates on dietary models of nonalcoholic fatty liver disease: current studies and insights. *Gene Expr*. 2018;18(1):5—17.
17. Nseir W, Hellou E, Assy N. Role of diet and lifestyle changes in nonalcoholic fatty liver disease. *World J Gastroenterol*. 2014;20(28):9338—9344.
18. Sheedfar F, Sung MM, Aparicio-Vergara M, et al. Increased hepatic CD36 expression with age is associated with enhanced susceptibility to nonalcoholic fatty liver disease. *Aging (Albany NY)*. 2014;6(4):281—295.
19. Torres-Villalobos G, Hamdan-Pérez N, Tovar AR, et al. Combined high-fat diet and sustained high sucrose consumption promotes NAFLD in a murine model. *Ann Hepatol*. 2015;14(4):540—546.
20. Kim MB, Lee Y, Bae M, et al. Comprehensive characterization of metabolic, inflammatory and fibrotic changes in a mouse model of diet-derived nonalcoholic steatohepatitis. *J Nutr Biochem*. 2020;85:108463.
21. Yang L, Roh YS, Song J, et al. Transforming growth factor beta signaling in hepatocytes participates in steatohepatitis through regulation of cell death and lipid metabolism in mice. *Hepatology*. 2014;59(2):483—495.
22. Katsarou A, Moustakas II, Pyrina I, Lembessis P, Koutsilieris M, Chatzigeorgiou A. Metabolic inflammation as an instigator of fibrosis during nonalcoholic fatty liver disease. *World J Gastroenterol*. 2020;26(17):1993—2011.
23. Wang JC, Gray NE, Kuo T, Harris CA. Regulation of triglyceride metabolism by glucocorticoid receptor. *Cell Biosci*. 2012;2(1):19.
24. Koorneef LL, van den Heuvel JK, Kroon J, et al. Selective glucocorticoid receptor modulation prevents and reverses nonalcoholic fatty liver disease in male mice. *Endocrinology*. 2018;159(12):3925—3936.
25. Marino JS, Stechschulte LA, Stec DE, Nestor-Kalinoski A, Coleman S, Hinds TD Jr. Glucocorticoid receptor β induces hepatic steatosis by augmenting inflammation and inhibition of the Peroxisome Proliferator-activated Receptor (PPAR) α. *J Biol Chem*. 2016;291(50):25776—25788.
26. Jiao Y, Zhao J, Zhang Z, et al. SRY-box containing gene 4 promotes liver steatosis by upregulation of SREBP-1c. *Diabetes*. 2018;67(11):2227—2238.
27. Lu Y, Liu X, Jiao Y, et al. Periostin promotes liver steatosis and hypertriglyceridemia through downregulation of PPARα. *J Clin Invest*. 2014;124(8):3501—3513.
28. Lemke U, Krones-Herzig A, Diaz MB, et al. The Glucocorticoid Receptor Controls Hepatic Dyslipidemia through Hes1. *Cell Metab*. 2008;8(3):212—223.
29. Rahimi L, Rajpal A, Ismail-beigi F. Glucocorticoid-induced fatty liver disease. *Diabetes Metab Syndr Obes*. 2020;13:1133—1145.
30. Verhague MA, Cheng D, Weinberg RB, Shelness GS. Apolipoprotein A-IV expression in mouse liver enhances triglyceride secretion and reduces hepatic lipid content by promoting very low density lipoprotein particle expansion. *Arterioscler Thromb Vasc Biol*. 2013;33(11):2501—2508.
31. Taylor AH, Raymond J, Dionne JM, et al. Glucocorticoid increases rat apolipoprotein A-I promoter activity. *J Lipid Res*. 1996;37(10):2232—2243.
32. Wang PW, Hung YC, Wu TH, Chen MH, Yeh CT, Pan TL. Proteome-based identification of apolipoprotein A-IV as an early diagnostic biomarker in liver fibrosis. *Oncotarget*. 2017;8(51):88951—88964.
33. Kuemmerle NB, Kinlaw WB. THRSP (thyroid hormone responsive). *Atlas Genet Cytogenet Oncol Haematol*. 2011;15(6):480—482.
34. Liu D, Wong CC, Fu L, et al. Erratum: squalene epoxidase drives NAFLD-induced hepatocellular carcinoma and is a pharmaceutical target. *Sci Transl Med*. 2018;10(460):1—16.

35. Sutti S, Albano E. Adaptive immunity: an emerging player in the progression of NAFLD. *Nat Rev Gastroenterol Hepatol*. 2020;17(2):81—92.
36. Luo Y, Burrington CM, Graff EC, et al. Metabolic phenotype and adipose and liver features in a high-fat western diet-induced mouse model of obesity-linked NAFLD. *Am J Physiol Endocrinol Metab*. 2016;310(6):E418—E439.
37. Schuster S, Cabrera D, Arrese M, Feldstein AE. Triggering and resolution of inflammation in NASH. *Nat Rev Gastroenterol Hepatol*. 2018;15(6):349—364.
38. Schuppan D, Surabattula R, Wang XY. Determinants of fibrosis progression and regression in NASH. *J Hepatol*. 2018;68(2):238—250.
39. Lu Y, Zhang Z, Xiong X, et al. Glucocorticoids promote hepatic cholestasis in mice by inhibiting the transcriptional activity of the farnesoid X receptor. *Gastroenterology*. 2012;143(6):1630—1640.
40. Vegiopoulos A, Herzig S. Glucocorticoids, metabolism and metabolic diseases. *Mol Cell Endocrinol*. 2007;275(1—2):43—61.